Dir 313
IR 78-1445

FILE COPY
DO NOT REMOVE

EA-6010-14
Dist. Category UC-90C

OCT 17 1979

MATERIALS RESEARCH FOR CLEAN UTILIZATION OF COAL

QUARTERLY PROGRESS REPORT

October - December 1977

Samuel J. Schneider
Project Manager

Institute for Materials Research
National Bureau of Standards
Washington, D. C. 20234

PREPARED FOR THE UNITED STATES
DEPARTMENT OF ENERGY

Under Contract No. EA-77-A-01-6010

"This report was prepared as an account of work sponsored by the United States Government. Neither the United States nor the United States Department of Energy, nor any of their employees, nor any of their contractors, subcontractors, or their employees, makes any warranty, express or implied, or assumes any legal liability or responsibility for the accuracy, completeness, or usefulness of any information, apparatus, product or process disclosed, or represents that its use would not infringe privately owned rights."

TABLE OF CONTENTS

		PAGE
I.	OBJECTIVE AND SCOPE OF WORK.	1
II.	SUMMARY OF PROGRESS TO DATE.	1
	Articles Published and Talks Presented	3
III.	DETAILED DESCRIPTION OF TECHNICAL PROGRESS	4
	1. Metal Corrosion.	4
	a. Constant Strain-Rate Test.	4
	b. Pre-Cracked Fracture Test.	16
	2. Ceramic Deformation, Fracture and Erosion. . . .	17
	3. Chemical Degradation	32
	a. Reactions and Transformations.	32
	b. Slag Characterization.	33
	c. Vaporization and Chemical Transport.	38
	4. Failure Prevention	40
	a. Failure Information Center	40
	b. Materials Properties Data Center	44

I. OBJECTIVE AND SCOPE OF WORK

Coal Gasification processes require the handling and containment of corrosive gases and liquids at high temperature and pressures, and also the handling of flowing coal particles in this environment. These severe environments cause materials failures which inhibit successful and long-time operation of the gasification systems. The project entails investigations on the wear, corrosion, chemical degradation, fracture, and deformation processes which lead to the breakdown of metals and ceramics currently being utilized in pilot plants. Studies will also be carried out on new candidate materials considered for improved performance. Special emphasis will be devoted to the development of test methods, especially short-time procedures, to evaluate the durability of materials in the gasification environments. These methods will focus on wear, impact erosion, stress corrosion, strength, deformation, slow crack growth and chemical degradation. A system has been initiated to abstract and compile all significant operating incidents from coal conversion plants as well as materials property and performance information important to the design and operation of these plants. This program will provide a central information center where problems of common interest can be identified and analyzed to avoid unnecessary failures and lead to the selection of improved materials for coal conversion and utilization. Active consultation to DOE and associated contractors will be provided as requested.

II. SUMMARY OF PROGRESS TO DATE

Brief Summary

1. Metal Corrosion

a. Constant Strain-Rate Test

The testing of specimens of 310 SS, 310s SS, 347 SS, 446 SS, Incoloy 800, and Inconel 671 was completed in a reducing coal gasification environment (CO-26%; CO_2-14.8%; H_2-26%; CH_4-10%; H_2S-1%; H_2O-22.2%) at temperatures of 450°C(840°F) and 600°C(1100°F) at a strain rate of $1 \times 10^{-6} s^{-1}$. The reducing environment did not seem to have a significant effect on the mechanical properties of any of the alloy specimens tested at 450°C(840°F) when compared to the mechanical property values of the alloy specimens tested in the helium environment at 450°C(840°F). The reducing environment at 600°C(1100°F) did have a significant effect on 310s SS and Incoloy 800 by reducing the values of the mechanical properties when compared to the data for the same alloys tested at 600°C(1100°F) in the helium environment. The effect of the reducing environment at 600°C (1100°F) on the other alloys did not seem to be significant. A thorough metallographic examination of the alloy specimens tested in helium, oxidizing, and reducing environments at 450°C(840°F) and 600°C(1100°F) is in progress.

During the next quarter, it is planned to complete metallographic examination of the alloy specimens. Also, it is planned to prepare a summary of the progress to date of the constant strain rate testing technique.

b. Pre-Cracked Fracture Test

The thermal-elastic stress intensity analysis has been completed for the wedge-loaded cantilever beam specimens. These results show that because the stress-intensity factor decreases significantly with increases in temperature for alloys of principal interest, such as stainless steels or Incoloys, this specimen configuration has limited applicability for reliable testing to determine the susceptibility to environmentally assisted stress-cracking.

More exact thermal-photo elastic stress analysis tests will be performed on the three specimen configurations described above as well as on a notched C-shaped specimen configuration.

2. Ceramic Deformation, Fracture and Erosion

A low-alumina refractory concrete has been exposed to a 70% H_2O - 30% CO_2 environment at temperatures of 510°, 710°, and 910°C and at pressures of 7.5 and 15.0 MPa. The room temperature flexural strength, compressive strength and erosion resistance of the concrete all increased after exposure. Work is continuing on construction and assembly of the high-temperature, high-pressure mechanical loader. A pressure balancing unit to regulate the pressure between the inner containment vessel and the outer pressure vessel is presently being installed.

3. Chemical Degradation

a. Reactions and Transformations

Over 60 energy dispersive powder diffraction patterns have been recorded from a bar of high alumina neat cement while it was being heated in a steam - CO_2 atmosphere. Significant changes were observed, and computer-assisted methods are being developed for use in completing the analysis. During the next quarter x-ray studies of high alumina cement in various atmospheres containing H_2O and CO_2 will continue, and the results will be correlated with those obtained under Task 2.

b. Slag Characterization

Construction of the high pressure-temperature viscosity apparatus has been completed and a synthetic slag has been melted in steam proving the adequacy of the heating system under pressure conditions.

c. Vaporization and Chemical Transport

A new gas handling system has been constructed and tested. Following resolution of a suspected reactor alignment problem, the thermodynamic effects of H_2O, SO_2 and O_2 on Na_2SO_4 transport will be investigated.

4. Failure Prevention

a. Failure Information Center

The Failure Prevention Information Center continued to enlarge its data collection activity. Seventy-four additional reports of operating experiences and failure analysis were received, classified, evaluated and entered into the data base. A detailed review of operating experiences at the Hygas plant and at the CO_2 acceptor plant was continued and will be completed during the next quarter.

b. Materials Properties Data Center

The establishment of the work and procedures of the Center continued with the formation of the library of contractors' reports, study of the formatting needs for a suitable computer system, investigation of computer data management systems, study of two series of contract reports, and preparation and revision of summary reports.

Articles Published and Talks Presented

J. W. Hastie arranged and chaired a session on "Metals in Combustion" at a Symposium on Metal Halide Vapors at the 152nd Meeting of the Electrochemical Society (Atlanta, GA, October 1977).

J. W. Hastie participated in a workshop on High Temperature Science and Solar Thermal Test Facilities (Albuquerque, New Mexico, November 1977).

J. W. Hastie participated in a workshop on High Temperature Chemical Kinetics: Applications to Combustion Research (NBS, December 1977).

J. H. Smith, "Failure Prevention at NBS," First International Conference on Materials for Coal Conversion and Utilization, October 11-13, 1977, National Bureau of Standards, Washington, D. C.

J. H. Smith, "Materials Failure Analysis," 9th Synthetic Pipeline Gas Symposium, sponsored by the American Gas Association, Chicago, Ill., October 31 through November 2, 1977.

J. H. Smith, "Materials Failure Analysis," published in the Proceedings of the 9th Synthetic Pipeline Gas Symposium, American Gas Association.

G. M. Ugiansky presented a talk, "Slow Strain Rate Stress Corrosion Testing in Coal Gasification Environments," at the First International Conference on Materials for Coal Conversion and Utilization held at NBS in October 1977.

J. L. Waring, R. S. Roth, W. S. Brower, and C. A. Harding, "Investigation of Calcium Aluminate Cement Phases Under High Gaseous Pressure," Journal of Research of the National Bureau of Standards, Volume 82, No. 3, November-December 1977.

III. DETAILED DESCRIPTION OF TECHNICAL PROGRESS

1. Metal Corrosion

a. Constant Strain Rate Test (G. M. Ugiansky and C. E. Johnson, 312.04)

Progress: Testing of specimens of 310 SS, 310s SS, 347 SS, 446 SS, Incoloy 800, and Inconel 671 was completed in the reducing coal gasification environment (CO-26%; CO_2-14.8%; H_2-26%; CH_4-10%; H_2S-1.0%; H_2O-22.2%) at temperatures of 450°C(840°F) and 600°C(1100°F) at a strain rate of 1×10^{-6} s^{-1}. The results of these tests at 450°C(840°F) and 600°C (1100°F) are shown in Tables 1 and 2 respectively.

It was previously shown (April-June 1977 Quarterly Progress Report and July-September 1977 Quarterly Progress Report) that an increase in test temperature from 450°C(840°F) to 600°C(1100°F) in ultra-pure helium environment and an oxidizing environment caused a significant change in the values of the mechanical properties* for the alloys tested. The same was noted for the reducing environment as seen in tables 1 and 2. This effect of increasing test temperature from 450°C(840°F) to 600°C(1100°F) can also be noted in the stress-strain curves in figures 1, 2, 3, 4, 5, and 6.

The effect of environment on the mechanical properties of the specimen alloys can be noted in tables 3, 4, and 5 and also in figures 1, 2, 3, 4, and 6. The values for the mechanical properties obtained in the helium environment (Table 3) are used as a base and the values for the mechanical properties obtained from the oxidizing (Table 4) and reducing (Table 5) environments are compared to that base. A significant effect caused by the environment is, at this point, arbitrarily set as a change of $\pm$ 10% in at least two of the three mechanical property values measured. The oxidizing environment (Table 4) had no significant effect on the mechanical properties of the specimen alloys tested at 450°C(840°F) with the exception of Inconel 671 which showed an increase in elongation and reduction in area while the tensile strength remained the same. The oxidizing environment had a significant effect by decreasing the values of the mechanical properties of specimens of alloys 310 SS, 446 SS, and Incoloy 800 when tested at 600°C(1100°F). The reducing environment (Table 5) had no significant effect on the mechanical properties of the alloy

*Mechanical properties — tensile strength, elongation, and reduction in area.

specimens tested at 450°C(840°F). The reducing environment did have a significant effect by decreasing the values of the mechanical properties of alloy specimens of 310s SS and Incoloy 800 when tested at 600°C(1100°F).

Metallographic examination of the alloy specimens tested in helium, oxidizing, and reducing environments at 450°C(840°F) and 600°C(1100°F) have been completed but not evaluated.

Plans: To further evaluate the results of testing in the oxidizing and reducing environments and prepare a summary of the results obtained to date by the constant strain rate test technique.

Table 1

Alloy Tests at 450°C(840°F) at a Strain Rate of 1 X 10^{-6} s^{-1} in the Reducing Environment*

Alloy	Tensile Strength MPa	Tensile Strength psi	Elongation %	RA %
310 SS	598	86,700	35.6	60.2
310s SS	513	74,400	38.8	69.9
347 SS	590	85,500	18.4	59.7
446 SS	574	83,200	21.0	58.0
In 800	551	79,800	34.3	70.5
In 671	676	97,900	38.0	39.3

*CO-26%, CO_2-14.8%, H_2-26%, CH_4-10%, H_2S-1.0%, H_2O-22.2%.

Table 2

Alloy Tests at 600°C(1100°F) at a Strain Rate of 1 X 10^{-6} s^{-1} in the Reducing Environment*

Alloy	Tensile Strength MPa	Tensile Strength psi	Elongation %	RA %
310 SS	362	52,500 (-39%)**	19.9 (-44%)	23.4 (-61%)
310s SS	336	48,700 (-35%)	30.3 (-22%)	33.8 (-52%)
347 SS	426	61,700 (-28%)	14.8 (-20%)	58.3 (-2%)
446 SS	160	23,200 (-72%)	49.5 (+236%)	83.3 (+144%)
In 800	353	51,100 (-36%)	32.7 (-5%)	61.7 (-12%)
In 671	448	64,900 (-34%)	16.3 (-57%)	16.8 (-57%)

*CO-26%, CO_2-14.8%, H_2-26%, CH_4-10%, H_2S-1.0%, H_2O-22.2%

**Note: The numbers in parentheses show the percent change in the mechanical property values with an increase in test temperature from 450°C(840°F) to 600°C(1100°F).

Table 3

Alloy Tests in Ultra-Pure Helium Environment at a Strain Rate of 1 X 10^{-6} s^{-1}

Alloy	Temp °C	Tensile Strength psi	Tensile Strength MPa	Elongation %	RA %
310 SS	450	87,300	602	37.9	64.6
	600	53,400	368	19.9	28.8
310s SS	450	75,100	518	38.9	63.7
	600	63,400	437	31.9	42.8
347 SS	450	82,300	568	18.8	65.2
	600	65,300	451	13.4	52.2
446 SS	450	85,000	586	17.3	57.0
	600	22,000	152	62.0	86.0
In 800	450	76,200	526	37.3	72.1
	600	67,700	467	37.1	60.1
In 671	450	98,600	680	32.8	37.7
	600	60,300	416	16.1	16.3

Table 4

Alloy Tests in Oxidizing Environment* at a Strain Rate of 1 X 10^{-6} s^{-1}

Alloy	Temp °C	Tensile Strength psi	Tensile Strength MPa	Elongation %	RA %
310 SS	450	84,200	581 (-3%)**	35.4 (-7%)	55.1 (-15%)
	600	50,300	347 (-6%)	14.0 (-30%)	21.6 (-25%)
310s SS	450	75,200	519 (0)	38.6 (-1%)	65.1 (+2%)
	600	54,500	376 (-14%)	32.8 (+3%)	43.9 (+3%)
347 SS	450	85,700	591 (+4%)	17.0 (-9%)	60.2 (-8%)
	600	66,600	460 (+2%)	14.5 (+8%)	46.0 (-12%)
446 SS	450	80,000	552 (-6%)	19.3 (+12%)	61.4 (+8%)
	600	15,800	109 (-28%)	34.7 (-44%)	88.3 (+3%)
In 800	450	78,900	544 (+3%)	32.6 (-13%)	65.8 (-9%)
	600	53,400	368 (-21%)	29.4 (-21%)	49.4 (-18%)
In 671	450	97,100	670 (-1%)	38.6 (+18%)	45.3 (+20%)
	600	57,600	397 (-5%)	17.5 (+9%)	20.7 (+27%)

*CO-11.6%; CO_2 - 15.4%; H_2 - 13.0%; CH_4 - 10%; H_2S - 1.0%; H_2O - 49%

**The numbers in parentheses in table 4 show the percent change in the mechanical property values caused by the oxidizing environment when compared to the results obtained for the same alloys tested in the ultra-pure helium environment (table 3).

Table 5

Alloy Tests in Reducing Environment* at a Strain Rate of 1 X 10^{-6} s^{-1}

Alloy	Temp °C	Tensile Strength psi	Tensile Strength MPa	Elongation %	RA %
310 SS	450	86,700	598 (-1%)**	35.6 (-6%)	60.2 (-7%)
	600	52,500	362 (-2%)	19.9 (0)	23.4 (-19%)
310s SS	450	74,400	513 (-1%)	38.8 (0)	69.9 (+9%)
	600	48,700	336 (-23%)	30.3 (-5%)	33.8 (-21%)
347 SS	450	85,500	590 (+4%)	18.4 (-2%)	59.7 (-8%)
	600	61,700	426 (-6%)	14.8 (+9%)	58.3 (+12%)
446 SS	450	83,200	574 (-2%)	21.0 (+21%)	58.0 (+2%)
	600	23,200	160 (+5%)	49.5 (-20%)	83.3 (-3%)
In 800	450	79,800	551 (+5%)	34.3 (-8%)	70.5 (-2%)
	600	51,100	353 (-24%)	32.7 (-12%)	61.7 (+3%)
In 671	450	97,900	676 (-1%)	38.0 (+16%)	39.3 (+4%)
	600	64,900	448 (+8%)	16.3 (+1%)	16.8 (+3%)

*CO-26%; CO_2 - 14.8%; H_2 - 26%; CH_4 - 10%; H_2S - 1%; H_2O - 22.2%

**The numbers in parentheses in table 5 show the percent change in the mechanical property values caused by the reducing environment when compared to the results obtained for the same alloys tested in the ultra-pure helium environment (table 3).

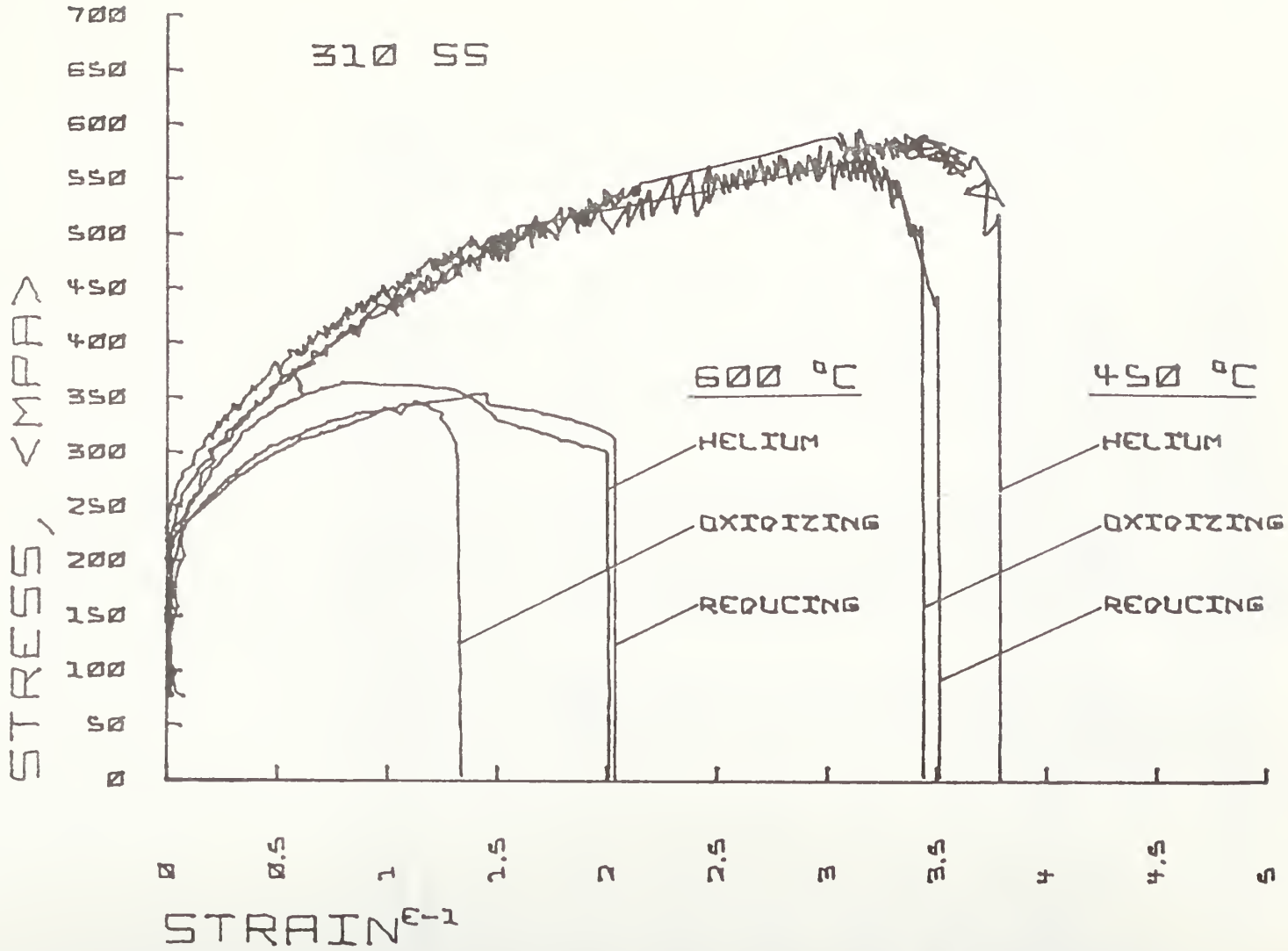

Figure 1. Stress-strain curves for 310 SS tested at 450°C(840°F) and 600°C(1100°F) in helium, oxidizing, and reducing environments at a strain rate of 1 X 10^{-6} s^{-1}. Stress (ksi) = $\frac{\text{Stress(MPa)}}{6.9\ \text{MPa/ksi}}$

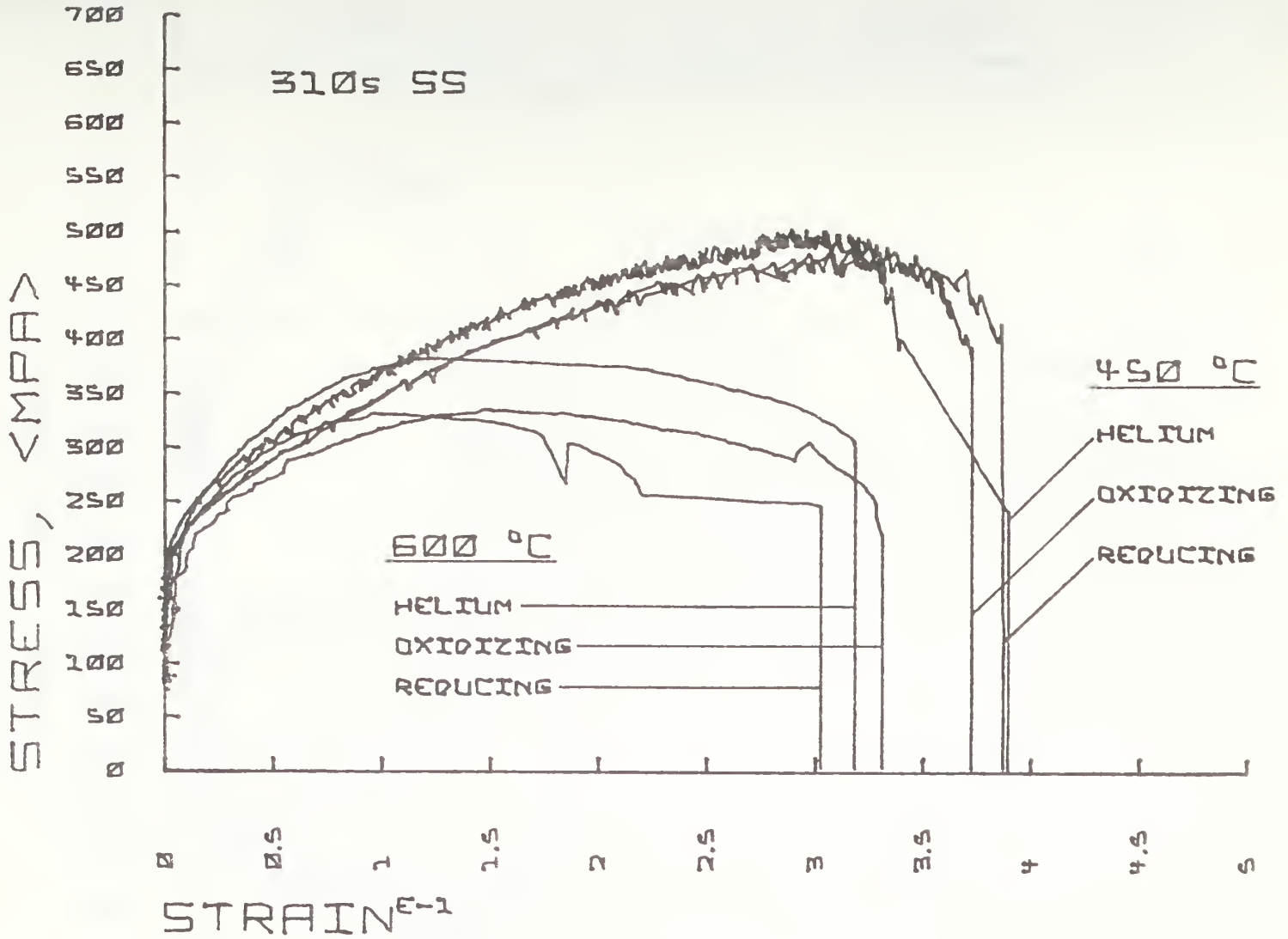

Figure 2. Stress-strain curves for 310s SS tested at 450°C(840°F) and 600°C(1100°F) in helium, oxidizing, and reducing environments at a strain rate of 1×10^{-6} s^{-1}. Stress (ksi) = $\frac{\text{Stress(MPa)}}{6.9\ \text{MPa/ksi}}$

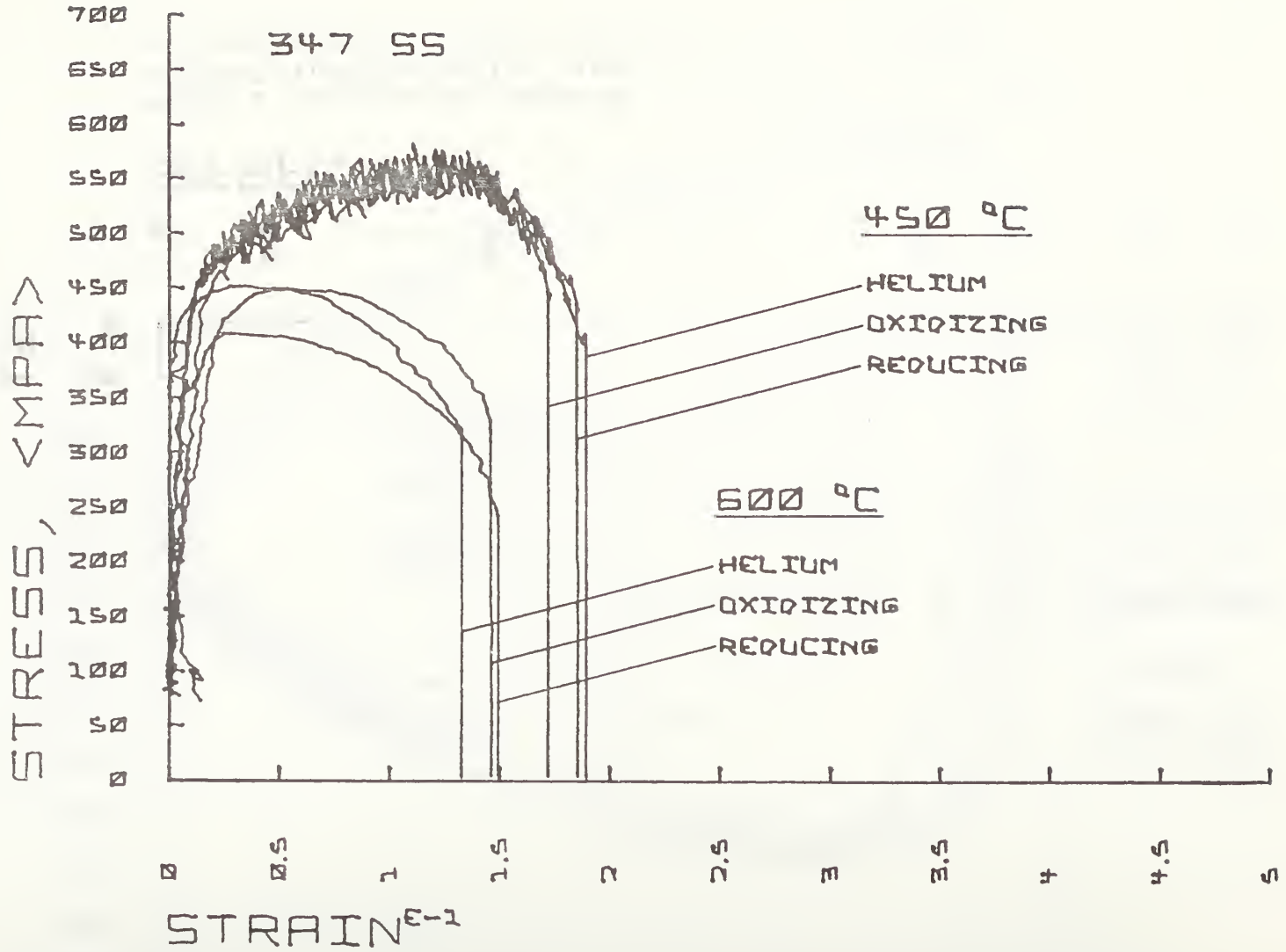

Figure 3. Stress-strain curves for 347 SS tested at 450°C(840°F) and 600°C(1100°F) in helium, oxidizing, and reducing environments at a strain rate of 1 X 10^{-6} s^{-1}. Stress (ksi) = $\frac{\text{Stress(MPa)}}{6.9\ \text{MPa/ksi}}$

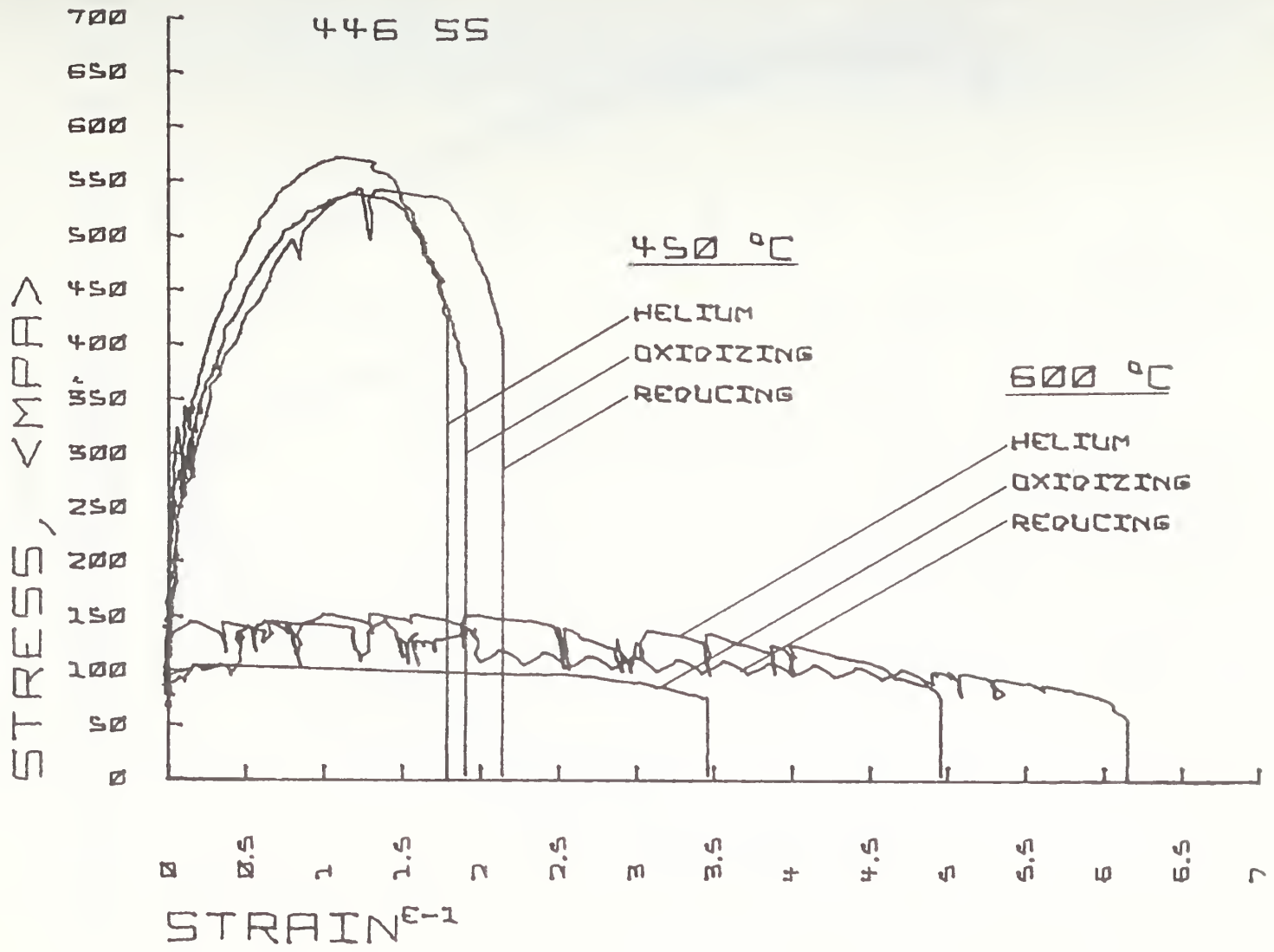

Figure 4. Stress-strain curves for 446 SS tested at 450°C(840°F) and 600°C(1100°F) in helium, oxidizing, and reducing environments at a strain rate of 1 X 10^{-6} s^{-1}. Stress (ksi) = $\frac{\text{Stress(MPa)}}{6.9\ \text{MPa}/\text{ksi}}$

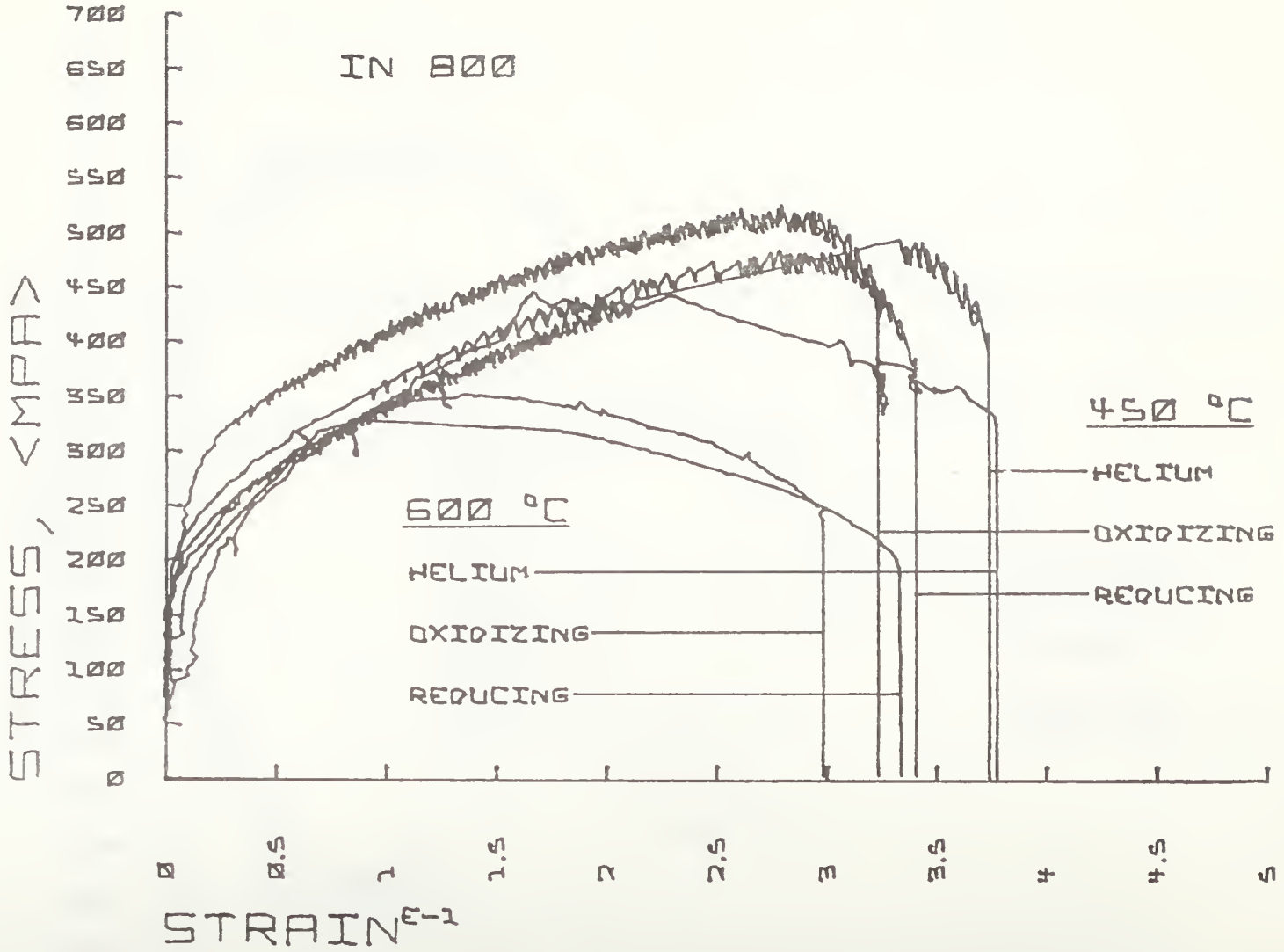

Figure 5. Stress-strain curves for Incoloy 800 tested at 450°C(840°F) and 600°C(1100°F) in helium, oxidizing, and reducing environments at a strain rate of 1 X 10^{-6} s^{-1}. Stress (ksi) = $\frac{\text{Stress(MPa)}}{6.9\ \text{MPa}/\text{ksi}}$

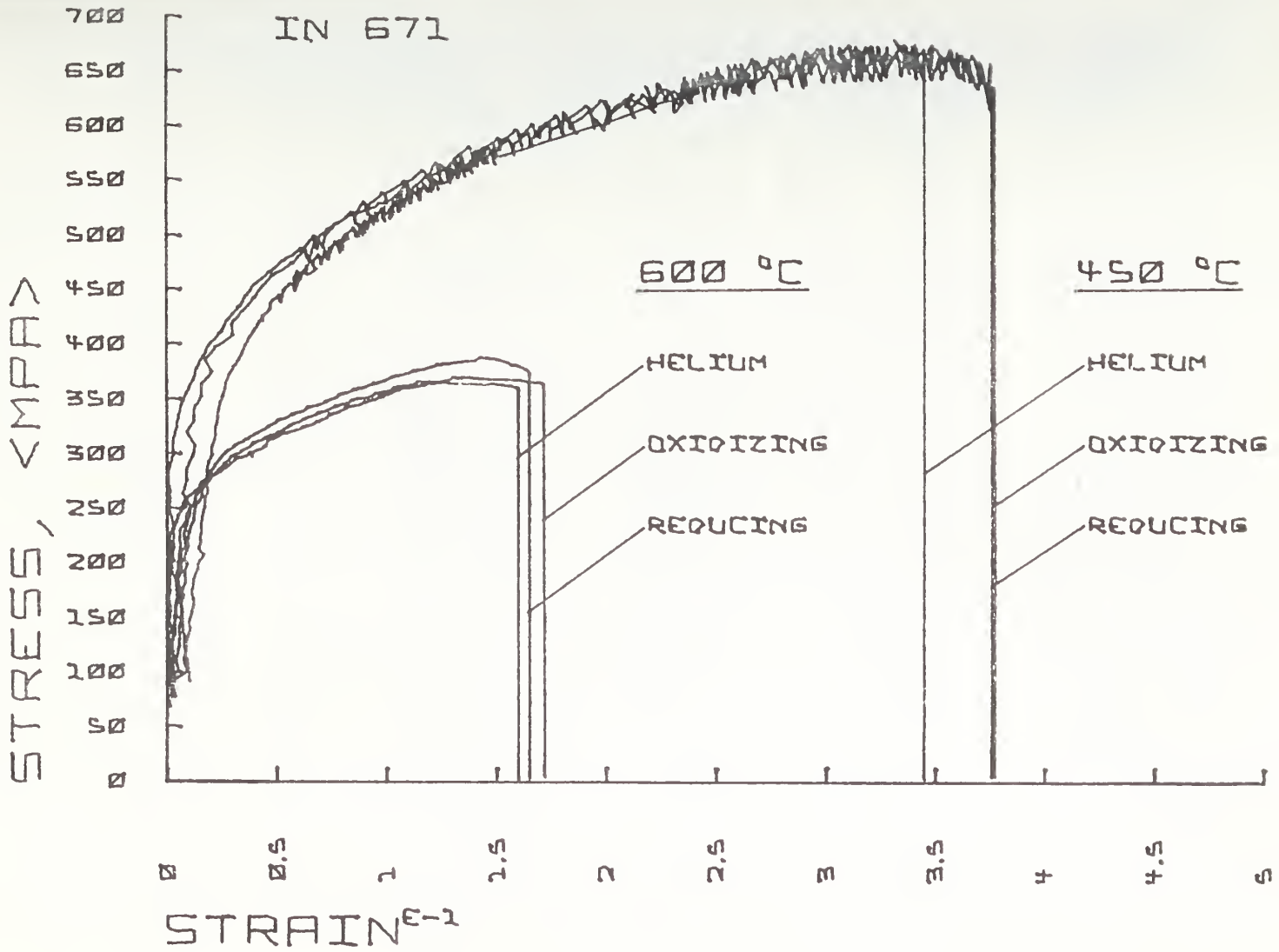

Figure 6. Stress-strain curves for Inconel 671 tested at 450°C(840°F) and 600°C(1100°F) in helium, oxidizing, and reducing environments at a strain rate of 1 X 10^{-6} s^{-1}. Stress (ksi) = $\frac{\text{Stress(MPa)}}{6.9\ \text{MPa}/\text{ksi}}$

b. Pre-Cracked Fracture Test (J. H. Smith, 312.01)

Progress: The thermal-elastic stress intensity analysis has been completed for the wedge-loaded cantilever beam specimens. These results show that because the stress-intensity factor decreases significantly with increases in temperature for alloys of principal interest, such as stainless steels or Incoloys, this specimen configuration has limited applicability for reliable testing to determine the susceptibility to environmentally assisted stress-cracking. This configuration should prove to be suitable for assessing the susceptibility to environmentally assisted stress cracking of non-metals or metals with a relatively low coefficient of thermal expansion that can be loaded with a wedge made of stainless steel.

Preliminary photo-elastic stress analysis experiments showed that a compression loaded double-edge notched specimen should prove to be suitable for use as an elevated temperature test specimen. By compensating for the decrease in elastic modulus with increase in temperature by differential thermal expansion of the loading fixture and the test specimen, a constant stress intensity with temperature should be obtained. However, the limitation of this specimen is that a more limited length of crack growth is possible than with the wedge loaded double cantilever beam specimens.

Preliminary photo elastic stress analysis tests were also conducted on a curved single edge notch beam specimen loaded as a bimaterial specimen. This specimen configuration appears to be suitable for elevated temperature tests and will permit testing for cracks propagating in the through thickness direction of piping and pressure vessels.

Plans: More exact thermal-photo elastic stress analysis tests will be performed on the three specimen configurations described above as well as on a notched C-shaped specimen configuration. Based on these tests, thermal-elastic stress analyses will be conducted to determine the stress-intensity factor on the optimum specimens. This thermal elastic stress analysis will then be extended to the elastic-plastic stress range typical of metals used at elevated temperature.

2. Ceramic Deformation, Fracture, and Erosion (E. R. Fuller, Jr., S. M. Wiederhorn, J. M. Bukowski, C. R. Robbins, and D. E. Roberts, 313.05)

Progress: Exposure studies on a low alumina (56%) refractory concrete in a 70% H_2O - 30% CO_2 environment were completed this past quarter. In this investigation, pre-fired* refractory concrete specimens were initially heated to the exposure temperature in an argon environment at atmospheric pressure. Once temperature equilibrium was reached, H_2O and gaseous CO_2 were metered into the exposure vessel to give the desired gas mixture and environment pressure. Samples were exposed to the H_2O - CO_2 environment at temperatures of 510°, 710° and 910°C and at pressures of 7.5 and 15.0 MPa. After an exposure period of 90 hours, the specimens were allowed to cool to 500°C at which point the exposure environment was slowly vented. By venting the exposure environment at 500°C, the formation on cool-down of low-temperature reaction products and their effects on subsequent room temperature mechanical property measurements were minimized. The room temperature flexural strength, compressive strength and erosion resistance for the low-alumina refractory concrete all increased after exposure to the 70% H_2O - 30% CO_2 environment (Table 1). X-ray diffraction analysis of samples exposed to the 70% H_2O - 30% CO_2 environment indicated the formation of CAS_2** at the expense of calcium aluminate phases (Table 2). It was found that the amount and crystallinity of CAS_2 seemed to increase both as a function of exposure temperature and environment pressure. As in earlier hydrothermal studies on the same low-alumina refractory concrete, it is the formation of the CAS_2 phase on exposure that is responsible for the increased strength and erosion resistance.

Exposure studies have also been initiated for a high-alumina (94%) refractory concrete in a simulated coal gasification environment. The ambient gas mixture being used is 40% H_2O, 25% H_2, 20% CO, and 15% CO_2 which gives a gaseous environment of H_2O, CO, CO_2, H_2 and CH_4 at the temperature-pressure exposure condition. Room temperature mechanical and mineralogical properties of exposed refractory concretes is presently in progress. Experimental observations have indicated mass transport of calcium from the refractory concrete being deposited as calcium carbonate (aragonite and vaterite) in cooler regions of the exposure vessel.

Work has continued on the development and the construction of the high pressure vessel for the mechanical testing of refractory concretes in simulated coal gasification environments. The load system has been

*1010°C - 5 hr.
**Cement Notation: C = CaO; A = Al_2O_3; S = SiO_2; H = H_2O

installed, and the operation of the hydraulic ram, bellows, and load cell has been checked by breaking castable refractory specimens at ambient temperature-pressure conditions. The resulting tests showed an excellent correlation in strength between specimens broken in the high-temperature, high-pressure mechanical loader and specimens broken on a commercial universal testing machine. The installation of a pressure regulating system which will balance the pressure between the inner containment vessel and the outer pressure vessel has begun. Minor modifications of the solenoid control valves used in the regulating system were found to be necessary in order to ensure rapid response to pressure imbalances. These modifications are presently being made and should be completed in a short length of time.

In a continuation of earlier work on the erosion of castable refractories, the erosion rate of a high density, calcined flint clay refractory has been investigated. Mean particle velocities of 72 m/s and 93 m/s were used in this study at temperatures of 25°C and 1000°C, respectively. As in previous work, erosion studies were conducted with 100 grit (150 μm) silicon carbide particles. The results of this study, figure 1, are compared with data obtained on a high alumina castable refractory, figure 2, and a phosphate bonded castable refractory, figure 3. The erosion rate is expressed in terms of mg of refractory eroded per gram of particles actually hitting the refractory surface. In all three cases, the rate of erosion was insensitive to impingement angle for angles ranging from 30 to 90°. For impingement angles of less than 15° a sharp decrease of erosion rate is suggested by some of the data. In absolute terms, the erosion rate measured at each angle of impingement was comparable for the three refractories studied, factors of less than two difference in the erosion rate being considered not significant. The similar appearance of the three sets of curves suggests a common mechanism of erosion for the three refractories.

As discussed in earlier reports, the rate of erosion of castable refractories is controlled mainly by the rate of wear of the cement holding the harder aggregate particles together. As erosion proceeds, channels are developed in the cement that bounds the aggregated particles, see figure 4, and when the channels have grown around the particles to a sufficient extent, the aggregate particles fall from the surface of the refractory. Channel formation in castable refractories occurs because the aggregate particles are much more erosion resistant than the cement matrix. The relative influence of cement versus aggregate wear can be demonstrated by conducting erosion measurements on the aggregate phase alone. A study of this type was conducted on two grades of high density aluminum oxide: one grade contained a 3-5 μm grain size; the other

contained a 30 μm grain size. Studies were conducted at temperatures of 25°C, 500°C and 1000°C over a velocity range ∿ 40 m/s to 120 m/s. The results shown in figure 5 may be compared with similar results on two types of castable refractory, figure 6, both of which contained aluminum oxide as the aggregate phase. We note that at equivalent velocity, the erosion rate of the refractories is approximately 1000 times that of the aggregate particles. It is for this reason that the erosion is due primarily to wear of the cement phase. It is also worth noting that the erosion rate of the aggregate is insensitive to temperature. This behavior differs from that of the castable, where erosion is temperature sensitive.

Channel formation in castable refractories accounts for the relative insensitivity of erosion rate to angle of impingement, since within each channel, impact occurs normal to the refractory surface, figure 4. However, when the angle of impingement decreases below a critical value, the cement phase will be protected by the aggregate from direct particle impingement and the rate of erosion will decrease. This process has been termed "shadowing," and because the erosion resistance of the aggregate particles of a castable is so much greater than that of the cement phase, the process of "shadowing" should occur commonly in refractories, and should provide an explanation for the shape of the wear versus impingement angle curves.

A model for "shadowing" was developed during the last quarter of this project. The model assumes that the surface aggregate particles can be approximated by spheres (figure 7) that are completely resistant to erosion, so that only the cement phase between the spheres is eroded by direct impingement of erosion particles. As the angle of impingement, α, decreases, the exposed area, S, of cement between particles decreases. From geometric arguments, figure 8, it can be shown that S is related to α and the relative aggregate particle radius R by the following formula: $S = 2(\sin\alpha - R)$, where it is assumed that the mean spacing between particles is 1, so that all results are obtained in terms of the unit spacing between aggregate particles. As the angle of impingement is decreased, a second geometric factor comes into play: the number of areas, S, exposed to the erosion beam increases so that the total available area, A, for erosion is given by the following formula: $A = 2(1-R/\sin\alpha)$. If it is now assumed that for any given mean particle velocity, the erosion rate is proportional to the exposed area of cement, then the erosion rate, E, is given by the following formula: $E/E_{90} = 2(1-R/\sin\alpha)$, where E_{90} is the rate of erosion at an impingement angle of 90°.

Theoretical curves for the relative erosion rate, E/E_{90}, are plotted in figure 9 as a function of impingement angle for various values of R. It is noted that for small values of R, the predicted curves are similar in

shape to the experimental curves. This finding suggests that the angular dependence of the erosion rate is determined by the size and spacing of the largest aggregate particles in the refractory. In the present study, the ratio of the aggregate particle size to aggregate separation distance would be expected to be about 0.1. This conclusion is qualitatively in agreement with the appearance of eroded surfaces studied in the present investigation.

Plans: Exposure studies will continue on both the high-alumina and the low-alumina refractory concretes in simulated coal gasification environments. Room temperature mechanical property measurements will be made and correlated to microstructural and mineralogical changes occurring in the concretes on exposure.

Construction of the high pressure vessel for mechanical testing in simulated coal gasification environments will be continued. The pressure regulating system will be installed and checked-out. On satisfactory operation of the regulating unit, the water injector will be installed and tested. At this point the mechanical loader should be operational, and systematic studies on refractory concretes can begin.

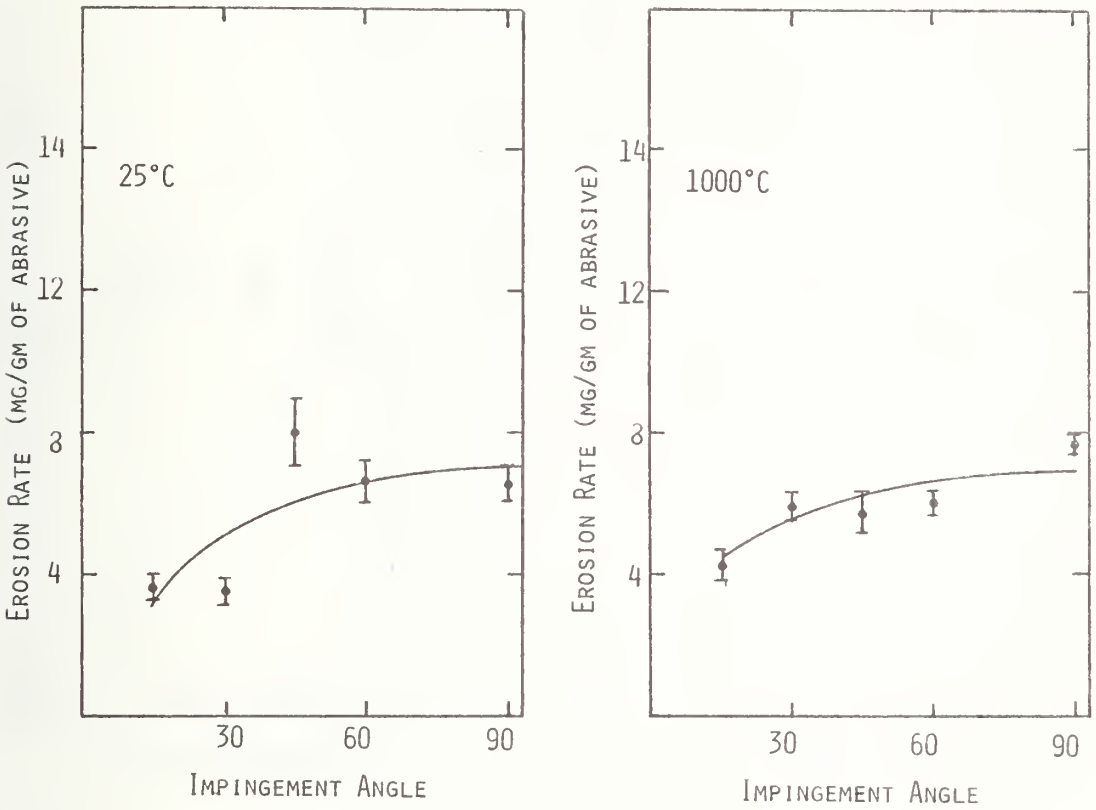

Figure 1. Effect of impingement angle on erosion rate: calcined flint clay castable; particle velocity = 72 m/s (25°C) and 93 m/s (1000°C).

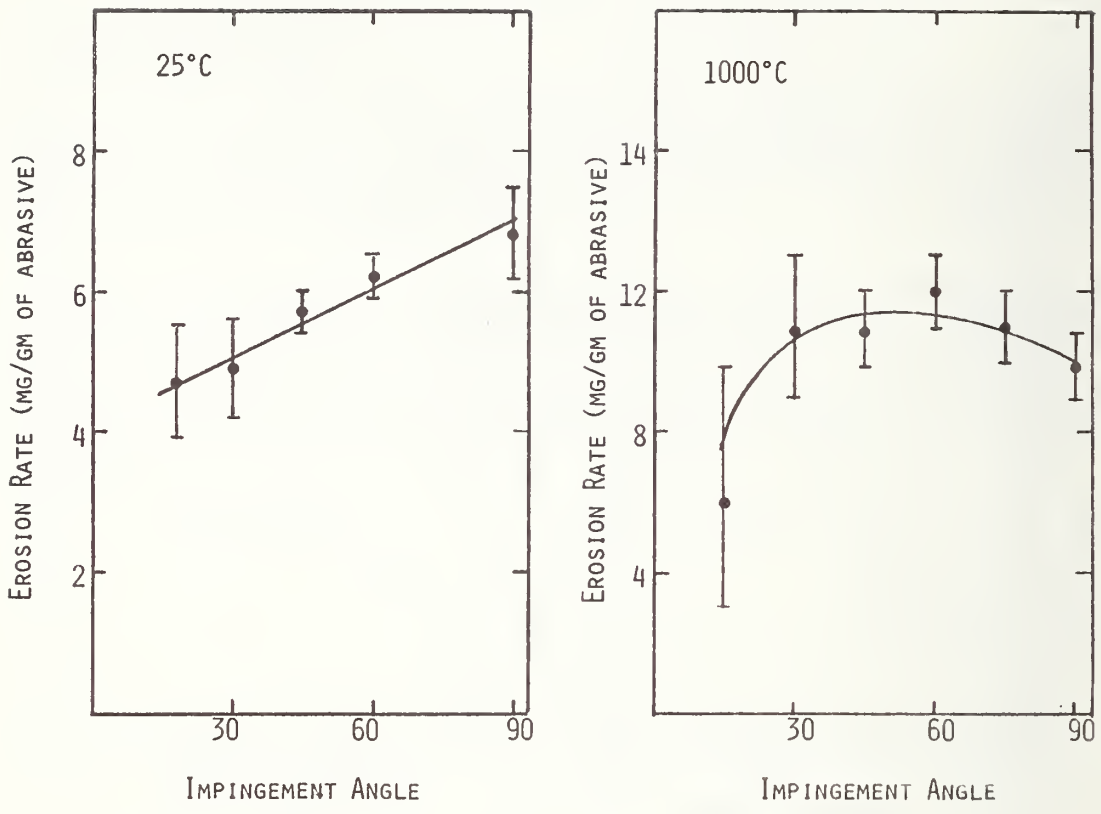

Figure 2. Effect of impingement angle on erosion rate: high purity alumina castable refractory; particle velocity = 72 m/s (25°C) and 93 m/s (1000°C).

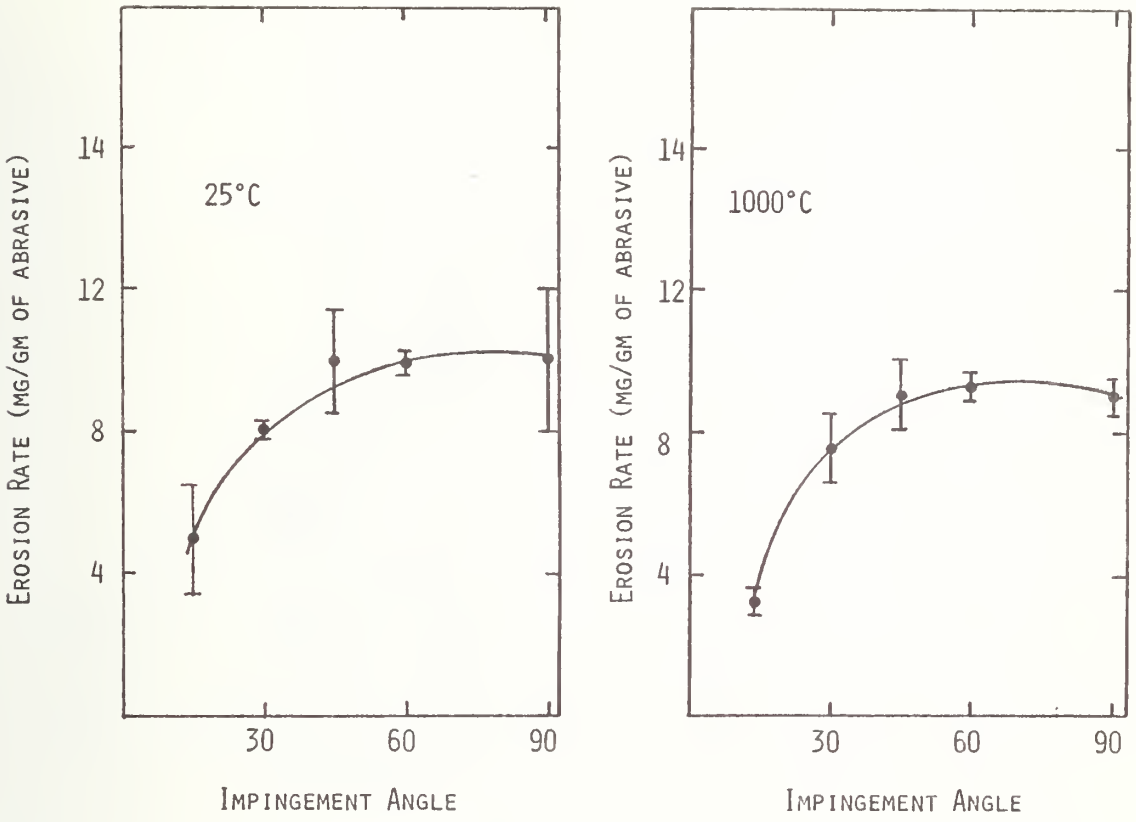

Figure 3. Effect of impingement angle on erosion rate: phosphate bonded castable refractory; particle velocity = 72 m/s (25°C) and 93 m/s (1000°C).

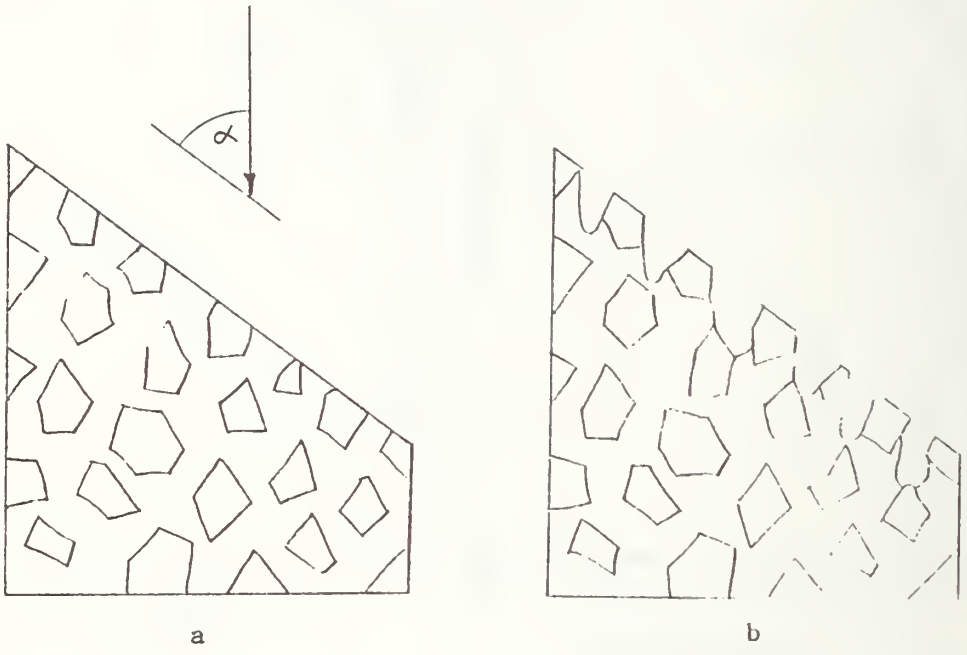

Figure 4. Schematic diagram of channel formation in castable refractories. a = original, b = eroded surface; α = angle of impingement.

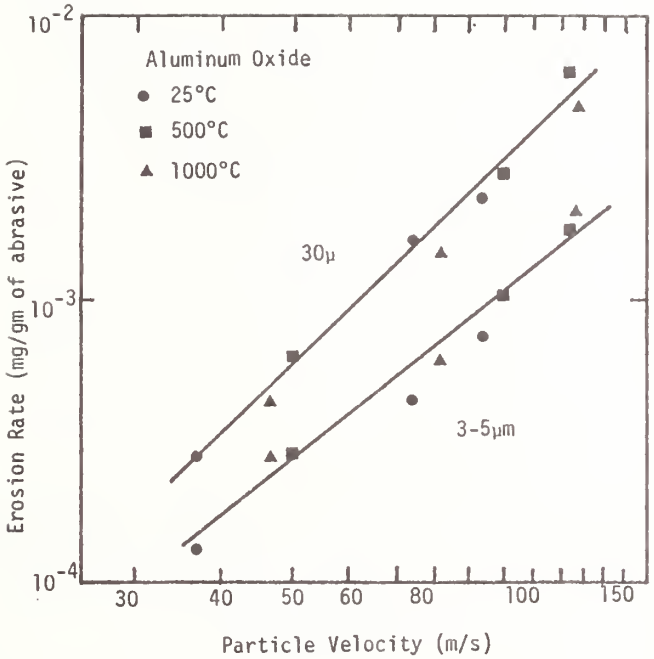

Figure 5. Erosion rate of high-density aluminum oxide ceramics as a function of temperature and particle velocity.

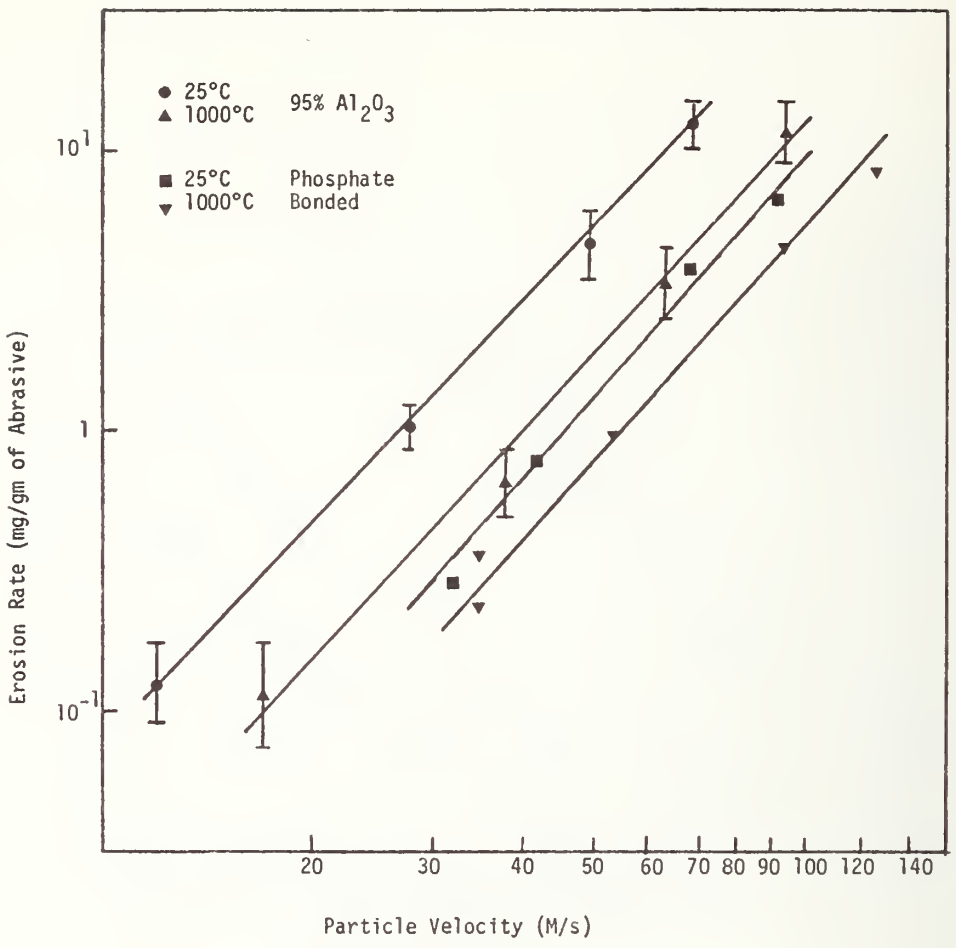

Figure 6. Erosion rate of two different castable refractories containing aluminum oxides as an aggregate phase.

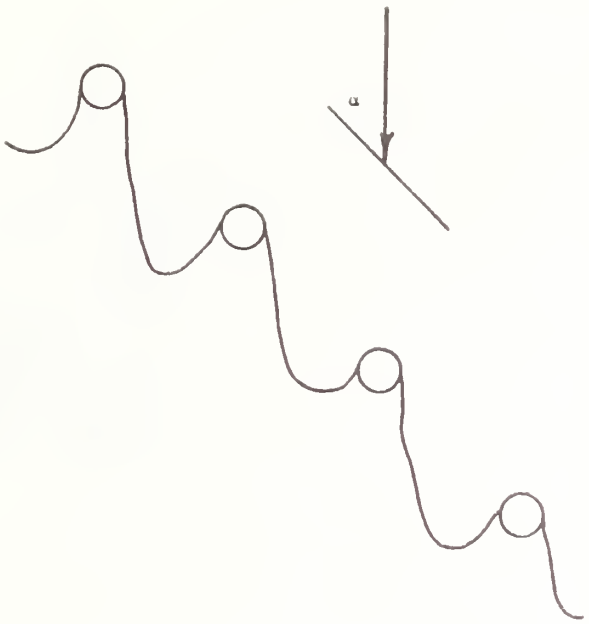

Figure 7. Model of the process of "shadowing," in which the aggregate particle protects the underlying cement.

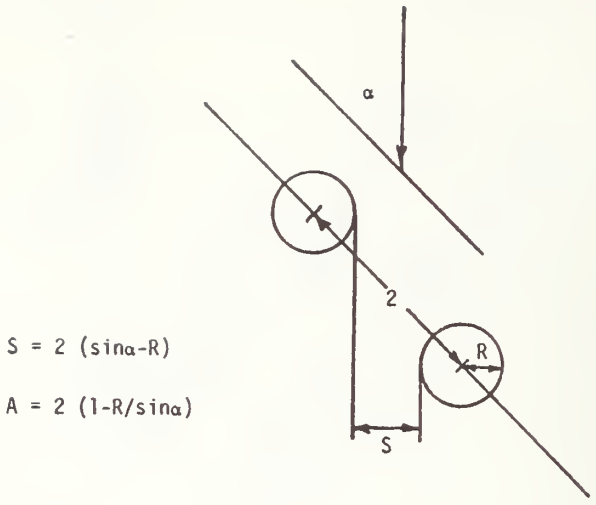

Figure 8. Geometric details of the model used to estimate the role of shadowing on the erosion process.

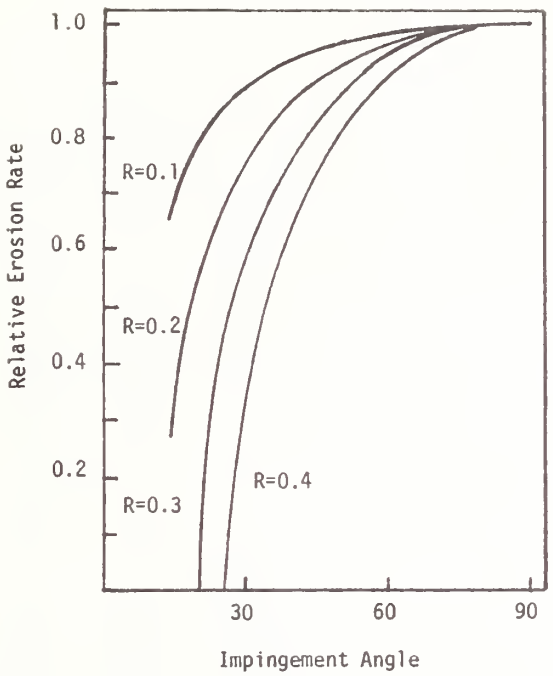

Figure 9. Theoretical prediction of relative erosion rate as a function of impingement angle.

Table 1. Room Temperature Mechanical Properties of a Low-Alumina (56%) Refractory Concrete after Exposure to a 70% H_2O - 30% CO_2 Environment. (Specimens prefired to 1000°C - 5 hr.)

	Flexural Strength (MPa)		Compressive Strength (MPa)		Erosion Resistance (mg/gm of abrasive)*	
Control	10.9 ±1.9		34.5 ±3.5		---	
Exposure Pressure	7.5 MPa	15.0 MPa	7.5 MPa	15.0 MPa	7.5 MPa	15.0 MPa
Exposure Temperature						
510°C	11.9 ±3.1	13.75 ±0.96	39.5 ±2.5	48.6 ±12.9	4.85	4.60
710°C	14.2 ±3.7	14.54 ±0.48	59.6 ±3.4	41.0 ±12.5	3.95	4.42
910°C	16.39 ±0.02	20.28 ±0.03	56.2 ±8.2	43.6 ± 5.5	3.75	4.51

*mg/gm - mg of specimen eroded per gm of abrasive hitting the specimen surface.

Table 2. X-Ray Diffraction Analysis of a Low-Alumina Refractory Concrete after Exposure to a 70% H_2O - 30% CO_2 Environment (Phases Listed in Apparent Order of Abundance).

Temperature °C	Exposure Time	Exposure Pressure 7.5 MPa	Exposure Pressure 15.0 MPa
Control	-	A_3S_2, Cristobalite, α-A, CA_2, CAS_2	
510	90 HRS	A_3S_2, Cristobalite, α-A, CAS_2, CA_2	A_3S_2, Cristobalite, CAS_2, α-A, CA_2
710	90 HRS	A_3S_2, Cristobalite, CAS_2, α-A, CA_2(tr), Tridymite (tr)	A_3S_2, Cristobalite, CAS_2, α-A, CA_2 (tr), Tridymite (tr)
910	90 HRS	A_3S_2, Cristobalite, CAS_2, CA_2(tr), Tridymite(tr)	A_3S_2, Cristobalite, CAS_2, α-A, CA_2(tr), Tridymite (tr)

3. Chemical Degradation of Ceramics

a. Reactions and Transformations (F. A. Mauer and C. R. Robbins, 313.06)

Progress: A bar of high alumina neat cement has been heated for 20 days in an H_2O-CO_2 atmosphere at temperatures and pressures up to 1000°C and 1000 psi. The composition of the atmosphere was approximately 80% H_2O - 20% CO_2 but varied considerably. In all, over 60 energy dispersive powder diffraction patterns were recorded. They indicate that significant reactions between the test specimen and the atmosphere occur. The hydration of CA_2, CA, and A to form compounds in the series C_3AH_6, AH_3, AH, and $C_4A_3H_3$, as well as the subsequent dissociation of these hydrates were observed. Because of the inherent low resolution of the energy dispersive powder diffraction patterns, changes are not as obvious as they would be in conventional powder patterns and individual reactions cannot be followed by visual inspection of the recorder charts. Fifty of the patterns have been recorded in digital form on punched paper tape so that computer assisted methods of interpretation can be used. We are now engaged in developing the software needed to process the digital data. At present it takes approximately 12 hours to read the 50 tapes into the computer for storage in a disc file and many problems arise because of flaws in the tapes. A method for transmitting the patterns directly to the computer is being sought so that the punched paper tape can be eliminated. Available plotting routines obtained are capable of plotting only 500 points. These are being modified so that the 1024 points recorded in each of our patterns can be plotted. Programs will then be written to subtract from each ordinate of a pattern the corresponding ordinate of the previous pattern and to plot the difference. The difference plot will be a sensitive indicator of changes in the intensities of diffraction lines. Plots will also be prepared to show the trend in intensity in selected channels corresponding to the diffraction peaks in the patterns prepared previously using pure reference standards. The number of counts in each of 5 diffraction peaks will be plotted for all of the 50 patterns in succession, and this will be repeated for each of the phases of interest. The plots will be useful for estimating the relative rates of transformation under various conditions. Other modes of analysis, as well as improved methods for presentation of data for reports are under consideration.

Additional components for recording process variables during x-ray studies have been received and will be installed during the next quarter.

Plans: Development of computer programs and improvements in the data logging equipment should be completed during the next quarter. Installation of additional equipment for controlling temperature and recording process variables is also expected to be completed. X-ray studies of high-alumina cement in various atmospheres containing H_2O and CO_2 will continue, and the results will be correlated with recent work done under Task 2.

b. Slag Characterization (W.S. Brower, J.L. Waring, C.A. Harding, 313.03 and D.H. Blackburn, 313.02)

Progress: The first prototype of the high pressure-temperature viscometer has been completed. Since the last reporting period the following have been added to the apparatus: new, platinum heater for melting slag, crucible for holding slag, pedestal to support crucible, shaft to rotate pedestal, suspension to be deflected, a sight port for viewing at ambient pressure.

After solving some difficult contact resistance problems, a synthetic slag was melted in high pressure steam, proving the adequacy of the heating system under pressure conditions.

Platinum Heater

The platinum heater (Figure 1) was fabricated from sheet .040" thick. It consists of a hollow right cylinder 2" I.D. and 4" long. To this cylinder at 180° were welded two large platinum tabs approximately .120" thick, 3 1/2" long x 4" high. These tabs are clamped into the electrodes. Another cylinder of alumina was cast around the platinum cylinder. The combination was fired at 1200°C for 24 hours. The outside circumference of the alumina cylinder was reinforced with platinum wire. This assembly was encased in refractory bricks which were shaped to accommodate the platinum-alumina cylinder. This additional brick insulation serves to insulate the heater and to minimize convective cooling by the steam on the thermocouple. This cooling effect was found to cause a temperature measurement problem in early experiments.

Crucible and Spindle

The platinum crucible used to contain the molten slag is 1 1/2" O.D. x 2 1/2" long with a 1/32" wall thickness. On the bottom of the crucible were welded tabs which form a cross pattern. These tabs are embedded into notches at the top of the alumina spindle. The alumina spindle is in turn clamped at the opposite end into the stainless steel rotating shaft. These precautions are necessary to prevent accidentally contacting the crucible with the heater. As an extra precaution a thin alumina liner is inserted between the rotating platinum crucible and the platinum heater.

Motor Driven Shaft

The stainless steel rotating shaft which supports the alumina spindle passes through the bottom flange. This shaft is sealed with two ethylene propylene O-rings. Outside the vessel the shaft is cooled

to prevent degradation of the O-rings. This cooling is accomplished by passing water through a jacket surrounding the shaft. The shaft is attached to the motor drive transmission by a universal coupling.

Sight Port and Suspension

Viscosity is to be measured in the following manner. The slag is placed in a crucible and melted, the bob is then immersed in the melt and the steam pressure is increased while the temperature is held constant until an appropriate temperature-pressure equilibrium is achieved. At this point the crucible is rotated and the angular deflection of a calibrated torsion member is observed. This deflection is proportional to the viscosity.

To make this type of measurement two modifications to the viscometer were made. The first was the introduction of a sight port so that the bob can be seen when immersed in the molten slag. The second modification is a method to lower the torsion suspension-bob to the desired height. To accomplish this a reciprocating shaft was introduced through a blank flange in the top of the vessel. The seal between the shaft and the flange is a viton-O-ring.

Problems

After assembling the various components and making preliminary heating experiments, some problems became apparent. When the system was operating at 1055°C and 130 psi steam, the platinum heater was using 18.48 KVA or approximately 4600 amps. With high currents and low voltages the various interfaces along the current path became extremely important. Originally the adjacent copper buses were made approximately flat and parallel and each mating surface was tinned. Voltage losses in the leads were noted as much as 60%. Some of this excessive loss was due to copper heating along the resistance path. The resistance of copper increases approximately 35% as the temperature increases from 20°C to 80°C. To reduce the effect of poor contacts, tin foil was sandwiched between all butting copper surfaces. The losses were measured and found to be approximately 15%. Additional water cooling was added at the junctions along the power leads. This cooling should keep the leads at approximately room temperature as the pressure vessel is heated.

Results

A synthetic slag with the composition SiO_2 42 wt%, Fe_2O_3 25 wt%, Na_2O 15 wt%, K_2O 5 wt%, MgO 5 wt%, Al_2O_3 3 wt% and CaO 5 wt% was melted at 1045°C and 135 psi of steam. After quenching the molten material under steam pressure and removing the crucible

from the pressure vessel the melted material was found to have formed a smooth concave meniscus. A significant weight gain of 8 mol % of H_2O was detected in the glass melt. This fused material was then reheated in air at 1000°C for approximately 30 min and found to foam (Figure 2). This is a clear indication that water was indeed present in the material. In this experiment no attempt was made to determine the maximum amount of water the molten slag can accommodate. However, it is clear that, in conjunction with viscosity measurements, data should be obtained concerning the maximum amount of H_2O incorporated in the molten slag versus time and temperature. Viscosity among other properties should be a function of the amount of water in the melt.

Plans: During the next quarter the viscosity of the previously melted synthetic slag composition will be measured in steam over a modest pressure range, from 15 to 100 psi. It will also be necessary to determine the time necessary to saturate the melt with respect to steam, this will be accomplished by making a series of viscosity measurements as a function of time at constant temperature and pressure until the viscosity becomes constant. When some insight is gained on the kinetics of steam solubility in the molten slag, then the viscosity measurements will be extended to the design pressure of the vessel ($\sim$ 300 psi).

Platinum Heater

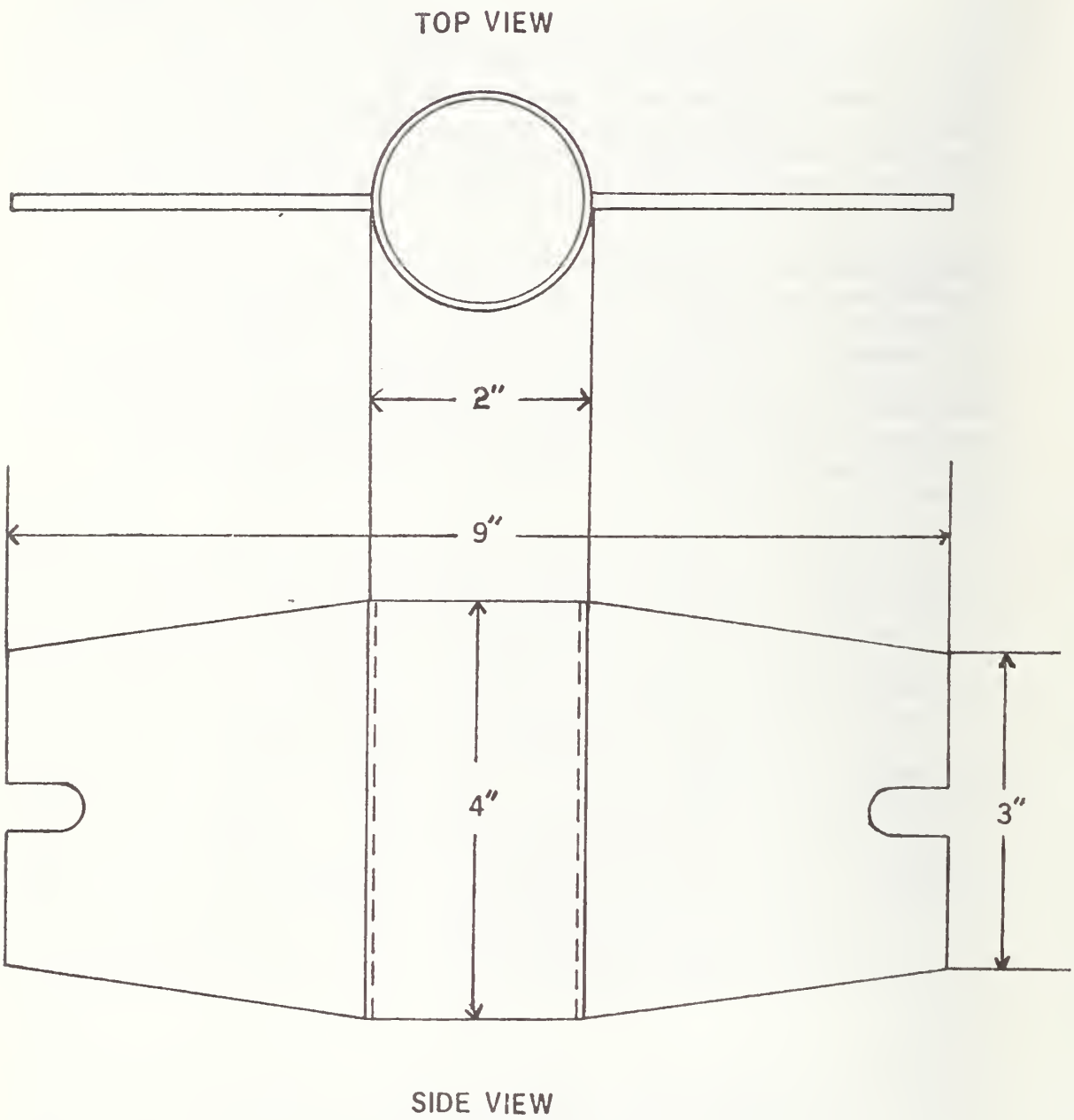

Figure 1. Platinum resistance element for heating slag container in steam.

SCALE: 5/8 IN =1 IN

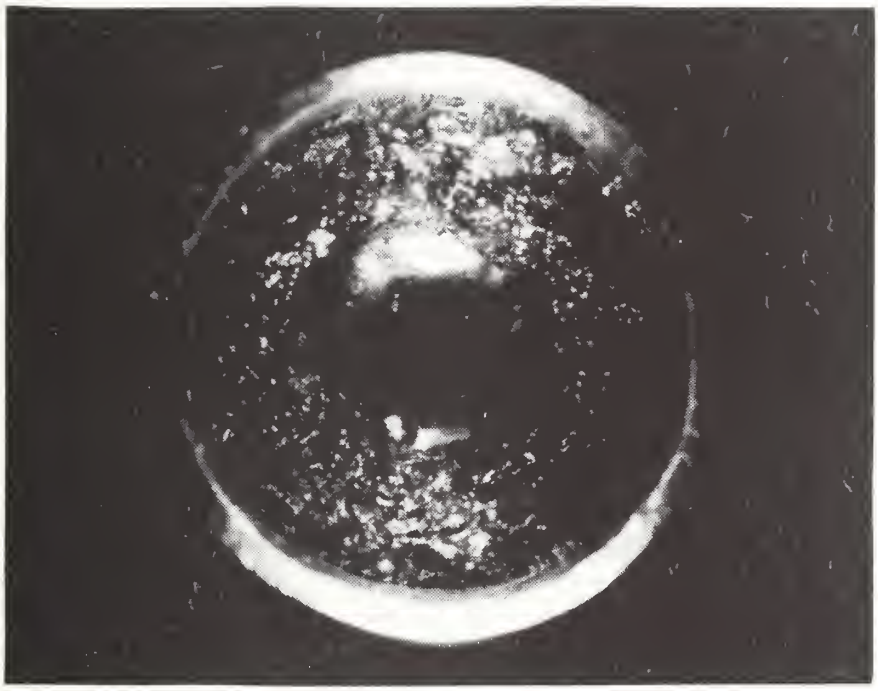

Figure 2. Remelted slag showing release of gas dissolved when melted in steam, crucible diameter ∿3/4 inch.

c. Vaporization and Chemical Transport (J. Hastie and D. Bonnell, 313.01)

Progress: A new gas handling system, incorporating three mass flow was constructed, calibrated and tested using H_2O, O_2 and SO_2 gases. Two of the flow controllers are of stainless steel construction and the third of monel. Gas flows between 0.4 - 5000 cc/min can be generated through these meters. This system is capable of handling any gaseous component (including corrosives) present in a coal gasification process and the composition of four of the constituent gases can be varied independently. Gas ratios varying from 0.5 to 100% are possible to a precision of better than 1% in the absolute concentration of any of the component gases. The system also enables rapid changes in mixture composition to be made during a series of experiments. Hence data can be obtained over a wide range of coal gas compositions for each substrate sample studied.

As a test of the gas handling system and the reactor's capability to faithfully sample a simple heterogeneous reaction system pertinent to corrosion in coal gasifiers, we initiated a study of the interaction of H_2O vapor with Na_2SO_4 liquid at temperatures of 800 - 1400°C and an H_2O partial pressure of 150 torr in an atmosphere of argon carrier gas. Under these conditions we expect, from the JANAF Thermochemical Tables, the following reactions to occur:

$$Na_2SO_4(\ell) = Na_2SO_4(g)$$

$$Na_2SO_4(\ell) + H_2O = 2NaOH + SO_2 + \frac{1}{2} O_2$$

$$\text{and } 2NaOH = (NaOH)_2.$$

However no mass spectra characteristic of the presence of NaOH, $(NaOH)_2$ or $Na_2SO_4(g)$ in the sample beam were found. As material deposits were noted in cooler regions of the reactor at the end of each experimental run, we know that some vaporization occurred. The inability to detect any vapor species by the molecular beam sampling process suggested a sudden breakdown in the reactor performance. To check the reactor's ability to handle and identify NaOH we introduced a pure sample of $NaOH(\ell)$ to the reactor. Mass spectra were obtained for the NaOH and $(NaOH)_2$ species at a temperature of 835°C. However the beam intensities were about a factor of 200 lower than expected, based on the known vapor pressure of NaOH and the calibrated sensitivity of the reactor-mass spectrometer system. That is, the NaOH pressure observed equals 1.3×10^{-5} atm as compared with the expected equilibrium pressure of 8.1×10^{-4} atm. Also, several attempts to monitor the vaporization of Na-containing species from a complex alkali-silicate mixture (components: $Na_2O/SiO_2/Na_2SO_4/Na_2CO_3/H_2O$) at temperatures in the region of 1000°C were unsuccessful. We believe that the sampler was defective during all of these experiments. The apparent drastic reduction in sample beam intensities could be due either to a change in the sampling cone-skimmer alignment during heating or to a change in the orifice geometry due to corrosion or deposition of nonvolatile material around the orifice. These possibilities are currently under investigation.

Plans: The possible misalignment of the high temperature reactor with the mass spectrometer will be investigated. If alignment changes during the experiment are observed the skimmer orifice will be enlarged to reduce the criticality of skimmer - sampling cone alignment. Also the mass spectrometer will be repositioned during experimental runs to optimize the ion source - skimmer alignment.

Due to the reactor performance problems encountered during the last quarter we still need to establish that the system is capable of faithfully sampling relatively simple heterogeneous systems. Of particular concern here is whether the sampling process disturbs the equilibrium composition that is expected for the simple systems using our operating conditions. If we can demonstrate that the sampling process does not appreciably alter the composition of the vapor sample, then any non-equilibrium phenomena found in subsequent studies of complex coal-gas-ceramic-slag-ash systems can be confidently attributed to the intrinsic properties of the particular chemical system under investigation. As was mentioned in our original proposal, a decision on whether the pressure range for study should be extended beyond the present 1-2 atm capability will be based on whether or not the coal gas-substrate reactions are intrinsically kinetically controlled. The modeling phase of our research program cannot readily be extended to actual coal gasifier pressures if kinetic phenomena are significant at the experimental conditions and if the experimental pressures differ from those in the gasifier. On the other hand if the reactions attain equilibrium at atmospheric pressure then they can be assumed to be at equilibrium at the higher pressures of coal gasifiers and thermodynamic models can be used.

Tests will therefore be resumed on the effect of H_2O, SO_2 and O_2 on alkali - metal transport. Reactions such as:

$$Na_2SO_4(\ell) = 2Na + SO_2 + O_2 \text{ and}$$

$$Na_2SO_4(\ell) + H_2O = 2NaOH + SO_2 + \frac{1}{2} O_2$$

will be monitored at constant temperature and variable partial pressures of H_2O, SO_2 and O_2. If the systems and the sampling process are at equilibrium then the equilibrium constants should be independent of partial pressure.

4. Failure Prevention

a. Failure Information Center (J. H. Smith, R. C. Dobbyn and W. A. Willard, 312.01) (W. S. Brower, 313.03)

Progress: During the quarter the Failure Prevention Information Center received 74 reports of operational experiences and components and materials failures in coal conversion pilot plants and process development units. This number includes several diagnostic failure analyses from Argonne National Laboratories and Oak Ridge National Laboratories. To date, the percent contribution of information items received from different coal conversion processes is shown in Table 1.

These reports have been classified and evaluated for technical completeness and accuracy and discrepancies have been resolved. Detailed abstracts of this information have been entered into the Center's computerized data bank. A recent update of the frequency of failure modes, which analyzes all information in the system, is shown in Table 2.

The Information Center continued to aid Battelle-Columbus in their preparation of the DOE Materials and Components Newsletter feature on failure experiences. Weekly updates of all abstracts are furnished to Battelle together with complete hard copy of certain reports when requested. During the quarter, the Center furnished 22 updated summaries and 38 complete reports.

The Information Center also handled 23 other requests for information during the quarter. In response to these inquiries, copies of 1,476 abstracts and several draft reports were transmitted. In addition, nine visitors to the Center were briefed on its scope, operation and future plans.

Additional reports required to complete the history of operating experiences at the Hygas plant have been obtained. This operation experience history will identify all components failures and operating events that caused disruption of the planned runs, and significant repairs or modifications. This review is being constructed from the available operating reports.

Direct contact with operating pilot plants, process development units and failure analysis laboratories continued. The BCR-Bigas plant submitted their first 16 failure reports and the Synthane, Hygas and Westinghouse processes continued their interaction with the Center.

Two presentations were made and one paper was published by J. H. Smith describing the operation of the Failure Prevention Information Center. R. C. Dobbyn participated in workshop discussions on recommended practices for evaluation of metals in high temperature, carburization environments.

Plans: The information gathering phase of this project will continue as more information is obtained from operating plants, process development units and failure analysis laboratories. Expanded interaction with other pilot plants and coal conversion technology centers is planned and will be completed as time permits. The operating experience history of the Hygas plant being constructed from the available operating reports will be completed.

Table 1

COAL CONVERSION PROCESSES

NO. OF ITEMS	PERCENT	PROCESS
7	1.44	ALL
1	0.20	BIGAS
1	0.20	BIOMASS
38	7.83	BMI
10	2.06	CARBONATE
19	3.91	CLEAN COKE
1	0.20	COED
73	15.05	CO2
2	0.41	CPC
2	0.41	EXXON
3	0.61	GFERC
67	13.81	HYGAS
1	0.20	LERC
23	4.74	LIGNITE
19	3.91	MERC
31	6.39	MISC.
1	0.20	ORNL
3	0.61	PERC
1	0.20	RANN
2	0.41	SEVERAL
34	7.01	SRC
4	0.82	SRC-W
106	21.85	SYNTHANE
4	0.82	SYNTHOIL
1	0.20	UNKNOWN
31	6.39	WESTINGHOUSE

485 + Total number of items in file

Table 2

NUMBER OF REPORTED INCIDENTS OF FAILURES
IN COAL CONVERSION PLANTS *,**

FAILURE MODE ANALYSIS

FAILURE MODE	PROCESS CO_2	HYGAS	SRC	SYNTHANE	OTHER	TOTAL
Corrosion	48	32	11	25	63	179
Aqueous	0	2	0	0	3	5
Carburization	10	2	0	0	5	17
Metal Dusting	4	0	0	0	3	7
Oxidation	4	3	0	0	5	12
Pitting	3	5	3	6	9	26
Sulfidation	16	11	0	7	4	38
General	11	9	8	12	34	74
Stress-Corrosion	6	5	5	5	32	53
Chloride	4	5	2	4	17	32
Other	2	0	3	1	15	21
Manufacturing Defect	14	10	13	22	37	96
Design	6	4	13	12	27	62
Fabrication	4	3	0	4	3	14
Quality Control	4	3	0	6	7	20
Equipment Malfunction	6	10	3	7	13	39
Overheat	6	10	3	4	11	34
Overstress	0	0	0	3	2	5
Erosion	7	7	11	21	38	84
Stress/Temp Failure	1	6	1	7	15	30
Creep	0	1	0	0	3	4
Fatique	0	2	0	4	10	16
Thermal Stress/Shock	1	3	1	3	2	10
Unknown	4	11	0	22	16	53

* Incidents reported to NBS Failure Prevention Information Center - Sponsored by DOE

** Operating times and levels of reporting vary with each plant

DATE: January 3, 1978

b. Materials Properties Data Center (H. M. Ondik, T. A. Hahn, 313.06, and I. J. Feinberg, 312.01)

Progress: The newly-established Materials Properties Data Center has the responsibility for designing and maintaining a data bank containing properties of materials for use in fossil energy applications. The program of the Center should provide for more rapid transfer of evaluated laboratory data and technological information, obtained by DOE-supported materials research, to designers of systems, materials researchers, and operating plants. The initial sources of information to be entered in the data bank are DOE contractors' reports of test data. Data from other sources will be added as appropriate. The data in the contractors' reports will be evaluated and summarized so as to provide the users with as much hard data in as brief a form as is possible. The data management system is being designed to be compatible with the Failure Prevention Information System, and to provide for appropriate search capabilities which will yield complementary information from both data banks. The information in the materials properties data bank will be made available to DOE and the fossil energy community in a variety of ways--reports, handbooks, and by direct query of the Data Center. Designing suitable means of distributing the information is listed among the duties of the Center.

During this first quarter the effort of the Center has been concentrated on establishing the basic operations of the Center. A library of the contractors' reports has been set up and will be expanded as more reports are written by and received from the contractors. The investigators have been studying the backlog of reports (which were catalogued earlier) to identify the type of information contained in them. The nature of the work requires a computer data management system which is open-ended in order to provide for the addition of new types of information as well as possible multiple entries from different sources for similar information. The system must have a matrix-type storage to provide for combination searches on varying sets of items so as to be responsive to users' needs and answer a variety of questions. There are package programs available with the necessary capabilities offered by various commercial groups. These groups are highly competitive and care must be taken to choose the best system. The system must be capable of handling numerical and textual information. Possibilities for storing and retrieving information in graphical form have been investigated and the flexibility available in terms of software and equipment is very encouraging. Enough of the data are in graphical form to make this feature desirable, even necessary.

The investigators have worked on specific sets of contractors' reports (one for refractories, one for alloys), studying and preparing evaluated summary tables and information statements. These first sets,

chosen somewhat randomly as test situations, have been valuable in providing necessary learning experience, indicating areas of activity in which our evaluation effort needs more detailed definition, and providing test examples of the format to be used in summarizing the reports. The summaries have been revised and new ideas and opinions have been formed by the investigators. Upon approval by DOE they will form a pattern for the summarizing of the rest of the reports. A catalogue file of the materials studied by the contractors is being prepared. Preliminary checks of the Oak Ridge Technical Information Center data bank have been made and differences found in comparing the list of reports in the DOE office files with the references cited in the TIC files.

Plans: Upon approval by DOE of the format and content of the first summary reports, further similar summaries of other contract work will be prepared and a means of distribution suggested to DOE. Catalogueing of the various materials being studied by the contractors and the designing of the computer file to contain the materials property data will continue. A full check of the ORNL TIC data base will be made.